LARGE-STROKE FLEXURE HINGES

Large-stroke flexure hinges inherently lose support stiffness when deflected, due to load components in compliant bending and torsion directions. To maximise performance over the entire range of motion, a topology optimisation suited to large-stroke flexure hinges has been developed to obtain an optimised design tuned for a specific application. This method was applied to two test cases, which has resulted in two hinge designs of unmatched performance with respect to the customary three-flexure cross hinge.

MARK NAVES, RONALD AARTS AND DANNIS BROUWER

Introduction

In high-precision manipulators, flexure-based mechanisms are often used for their deterministic behaviour, which is due to the absence of friction, hysteresis and backlash. However, when designing flexure hinges, designers face a trade-off between flexibility for motion in certain desired directions, and stiffness to constrain motion for guiding in the remaining directions. Typical flexure hinges have a range of about 10°, beyond which the guiding stiffness and load-bearing capacity decrease dramatically. Consequently, it is not a minor thing to design flexure hinges suited to large-stroke applications. By using a topology optimisation suitable for large deflections, guiding stiffness can be greatly increased for flexure hinges vastly exceeding a 10° range of motion.

Typical structural topology optimisations are often based on density distribution functions, which divide the design domain into a large number of finite elements and employ piecewise constant 'element densities' in each of the finite elements as the design variables. This method shows good results for small deformations. However, when more complex three-dimensional topologies are considered, the design domain becomes very large and topological optimisations can become computationally intensive. Furthermore, geometrical nonlinearities are mostly disregarded, as they significantly increase computational load, and often iterative solvers are required, which have the potential to fail to converge. This makes finite-element modelling currently impractical for optimising three-dimensional large-stroke flexure mechanisms including the required nonlinear effects.

To overcome the limitations of existing optimisation strategies, a new multibody-based topology synthesis method has been developed for optimising large-stroke flexure hinges. This topology synthesis consists of a layout variation strategy based on a building-block approach combined with a shape optimisation in order to obtain the optimal design tuned for a specific application.

Topology synthesis method

The topology synthesis begins with a shape optimisation of an initial reference layout, which is capable of obtaining an acceptable level of performance. For this initial layout, the customary three-flexure cross hinge (TFCH) is used, schematically illustrated in Figure 1.
The goal of this shape optimisation is to obtain the optimal geometrical shape (flexure thickness, width, length, etc.) that will provide maximum support stiffness for the application considered. To obtain the optimal shape, a parameterised description of the flexure hinge is used, where an optimisation algorithm searches for the optimal set of design parameters, taking all constraints into account (in the example given, maximum stress and required stroke).

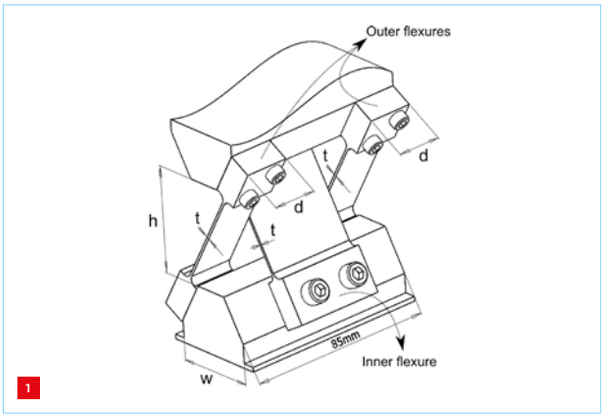

1 *Parameterised model of a three-flexure cross hinge (TFCH).*

AUTHORS' NOTE

Mark Naves, Ph.D. student, and Dannis Brouwer, Professor, are members of the chair of Precision Engineering, and Ronald Aarts, Associate Professor, is a member of the chair of Structural Dynamics, Acoustics & Control, all in the Department of Mechanics of Solids, Surfaces & Systems at the University of Twente, the Netherlands.
Some of this work was presented at the 17th euspen Conference & Exhibition on 30 May - 2 June 2017 in Hannover, Germany.

m.naves@utwente.nl
www.utwente.nl/en/et/ms3

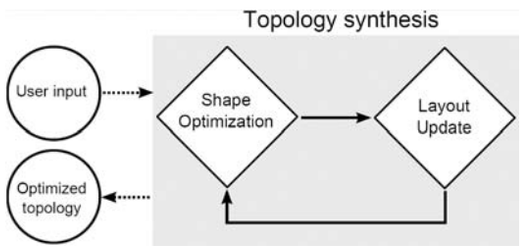

2

The performance of a specific set of design parameters is numerically evaluated with the flexible multibody program SPACAR [1], which uses a series of interconnected nonlinear finite-beam elements. The flexibility of these elements is naturally included in the formulation, owing to a specific choice of discrete deformation modes. Therefore, only a limited number of elements is required to produce fast and accurate results. After the optimal shape of the initial reference is obtained, the layout is updated to improve support stiffness, and the newly obtained layout is re-optimised. In an attempt to find the optimal solution, this process of consecutive shape optimisation and layout update is repeated. This strategy is schematically illustrated in Figure 2.

Building-block approach

In order to obtain the optimal flexure layout, a number of compliant 'building blocks' are defined to synthesise the layout effectively [2]. With each layout update, a building block is replaced or added in order to try to improve support stiffness, based on the typical stiffness properties of each building block and the critical support stiffness from the antecedent shape optimisation. Three building blocks are combined to construct a single flexure hinge: one building block at the inner position of the flexure hinge (in the example, the middle leaf spring of a TFCH); and two identical building blocks at the outer position of the flexure hinge (Figure 1).

The building blocks used to update the layout are a leaf spring (LS), a torsionally reinforced leaf spring (TRLS) and a three-flexure cross hinge (TFCH). Each building block is schematically shown in Figure 3. An overview of the typical stiffness properties at a deflected state of each building block is given in Table 1. Numerical values of the directional support stiffness (defined as the resistance to deformation in a specific direction while motion in all other directions is constrained) for each building block – given a building block width of 20 mm, height of 50 mm, flexure thickness of 0.5 mm, E-modulus of 210 GPa and deflection angle of 0.6 rad – are presented between parentheses. Note that these values are affected by selected geometry and material properties. However, they do provide a proper indication of the typical stiffness characteristics of each building block.

Table 1. Stiffness properties of building blocks in a deflected state.

	LS	TRLS	TFCH
Support stiffness			
x-translation [N/mm]	– (4.1)	– (8.6)	+ (120)
y-translation [N/mm]	– (41)	– (8.2)	+ (290)
z-translation [N/mm]	+ (6,600)	+ (6,700)	– (650)
x-rotation [Nm/rad]	– (48)	+ (1,400)	– (31)
y-rotation [Nm/rad]	– (5.6)	+ (1,300)	– (16)
Motion compliance			
z-rotation [rad/Nm]	+ (13)	– (0.49)	+ (13)

Leaf spring (LS)

The first building block considered is the customary leaf spring (Figure 3a). This element typically has only limited support when considering the stiffness properties in its deformed state, except for translational stiffness in *z*-direction. Furthermore, it provides high compliance in the desired degree of freedom (*z*-rotation).

Torsionally reinforced leaf spring (TRLS)

In order to improve torsional stiffness around the *y*-axis and in-plane bending stiffness around the *x*-axis, the so-called torsionally reinforced leaf spring (Figure 3b) is presented, which is inspired by the infinity hinge [3]. This building block consists of a single central leaf spring reinforced with one or more folded leaf springs to improve torsional and in-plane bending stiffness. Motion compliance in the degree of freedom is reduced due to the added folded leaf springs.

Three-flexure cross hinge (TFCH)

The third building block, which aims to increase translational stiffness in *x*- and *y*-direction over the range of motion, is a three-flexure cross hinge (Figure 3c). Two TFCHs can be stacked in series to form the so-called double TFCH (DTFCH), which provides increased translational support stiffness.

2 *Schematic representation of the topology synthesis method.*

3 *Deflected flexural building blocks used to 'synthesise' flexure layout. (a) LS. (b) TRLS. (c) TFCH*

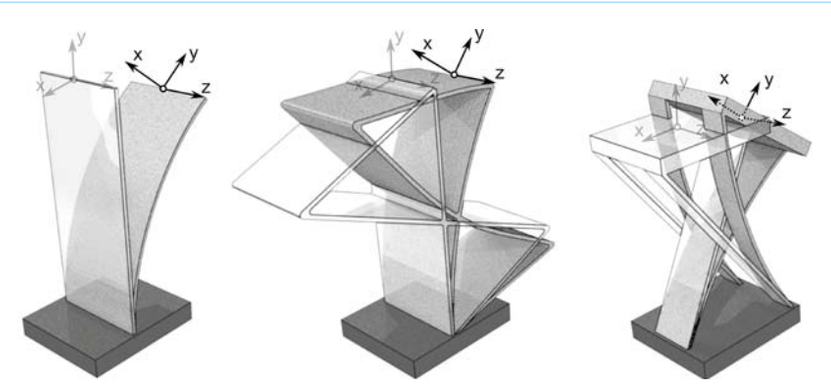

3

Optimisation examples

In order to illustrate the applicability of the suggested method, two optimisation cases will be discussed, aimed at maximisation of directional support stiffness and the first parasitic frequency for a specific mechanism, respectively. Steel was selected as the material, to demonstrate the achievable performance and to facilitate comparison with previous studies [3]. However, this choice does hamper comparison with the experimental validation; see below. For both cases, an allowable stroke of –45° to +45° deflection is considered and the maximum width is bounded to 85 mm. Furthermore, the allowable stress for steel is limited because of deformation to 600 MPa, about one third of the yield stress.

Case 1

The aim is to optimise the support stiffness orthogonal to the axis of rotation (for this case, the vertical support stiffness). The support stiffness for the shape-optimised initial reference layout (the TFCH consisting of leaf springs for the inner and outer building block) decreases to 250 N/mm at a maximum deflection angle, which is less than 1% of the stiffness without deflection. The final optimised layout after two layout updates, consisting of a DTFCH for both the inner and outer building block, shows a minimum support stiffness of 2,100 N/mm over the range of motion, which results in an increase in performance of about a factor eight. Figure 4 displays a prototype resulting from the optimised topology, made of DuraForm PA (Nylon) and manufactured with selective laser sintering (SLS). An overview of the support stiffness for intermediate shape optimisations is given in Table 2.

Table 2. Support stiffness for intermediate shape optimisations of Case 1.

Iteration	Outer building block	Inner building block	Minimum support stiffness (45° deflection) [N/mm]	Maximum support stiffness (0° deflection) [N/mm]
1	Leaf spring	Leaf spring	250	88,000
2	Leaf spring	DTFCH	800	41,000
3	DTFCH	DTFCH	2,100	63,000

Case 2

An optimisation is performed aimed at maximising the first parasitic frequency of the mechanism presented by Folkersma et al. [4]. In short, the flexure hinge considered for this application is subjected to a mixed load of inertia ($I_{xx} = 3.8{\cdot}10^{-3}$, $I_{yy} = 3.5{\cdot}10^{-2}$, $I_{zz} = 3.8{\cdot}10^{-2}$) and mass ($m = 0.57$ kg), concentrated in the pivot of the joint, where most emphasis is put on the inertial load. Table 3 gives an overview of the minimum parasitic frequency over the range of motion of each optimised layout at each layout update step. The first parasitic eigenfrequency for the shape-optimised initial reference (again the TFCH consisting of leaf springs for the inner and outer building block) decreases down to 10 Hz, which is about 7% of the frequency without deflection. The final optimised layout, consisting of six reinforced leaf springs stacked in series supported by two DTFCHs at either side of the joint, shows a minimal parasitic frequency of 100 Hz, which is an increase of about a factor ten in parasitic frequency. Figure 5 shows a prototype resulting from the optimised topology.

For a step-by-step animation of this optimisation case, see [5] and the Appendix below.

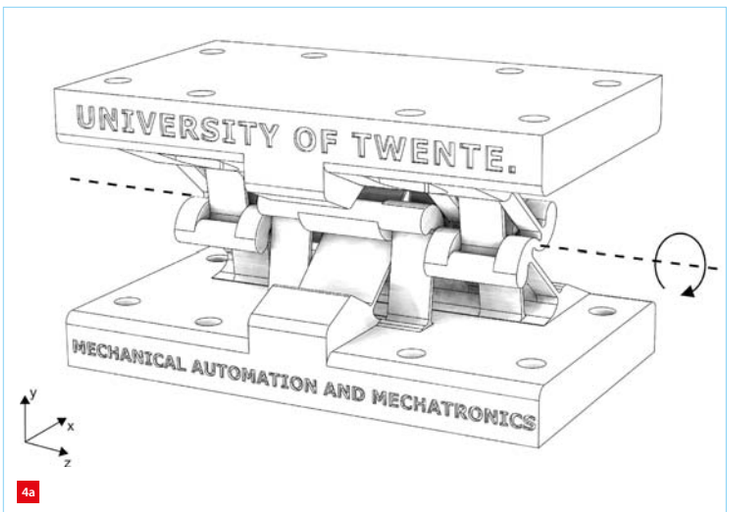

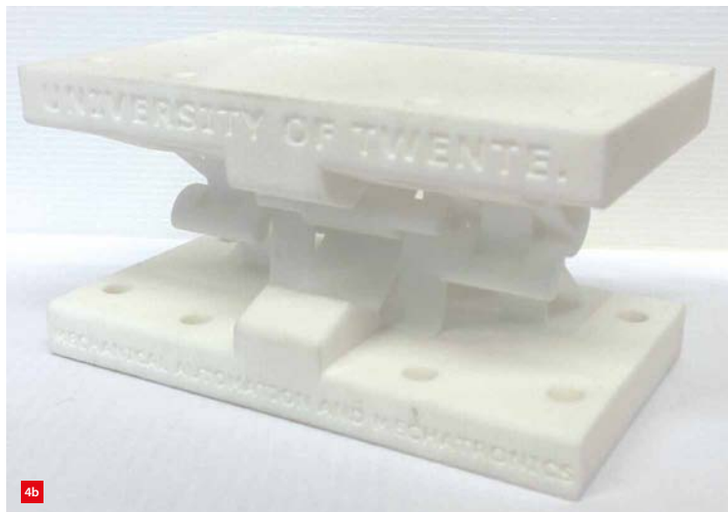

4 *Optimised flexure hinge for Case 1.*
(a) CAD rendering.
(b) Realisation.

Table 3. Frequency of first parasitic mode for intermediate shape optimisations of Case 2.

Iteration	Outer building block	Inner building block	Minimum parasitic frequency (45° deflection) [Hz]	Maximum parasitic frequency (0° deflection) [Hz]
1	Leaf spring	Leaf spring	10	150
2	Leaf spring	TRLS (1x)	14	56
3	Leaf spring	TRLS (2x)	39	154
4	DTFCH	TRLS (2x)	43	203
:	:	:	:	:
8	DTFCH	TRLS (6x)	100	132

Experimental validation

To validate the models that are used for evaluating the performance of the flexure hinges, an experimental validation has been conducted. For this validation, the optimised flexure hinge of Figure 5 was used. For practical reasons (options like assembling various wire-eroded metal parts or metal 3D-printing are not straightforward), this flexure hinge was made of DuraForm PA and manufactured with SLS. Furthermore, due to the different material properties of Nylon with respect to steel and the geometrical limitations with respect to the sintering process, the flexure thickness is increased to at least 0.7 mm to comply with the SLS Nylon additive manufacturing technology. These experimental changes have been accounted for in the simulations.

To verify the results, a series of measurements were performed to confirm the frequencies of the first four disturbing vibrating modes of interests. Figure 6 shows the measurement set-up for measuring rotational modes around the x-axis. To measure the eigenfrequencies over its entire range of motion, the hinge was held in a deformed state by a wire flexure to prevent any interaction with the considered eigenmodes. These measurements were repeated over the entire range of motion in steps of 5°, where a protractor was used to obtain the deflection angle.

An overview of the experimental results over the entire range of motion is given in Figure 7. The frequency of the first disturbing mode, consisting of a rotation around the x-axis, shows a good agreement with the model results. The second and third disturbing mode, consisting of translations in the x- and y-direction, and the fourth disturbing mode,

5 *Optimised flexure hinge for Case 2. (a) CAD rendering. (b) Realisation.*

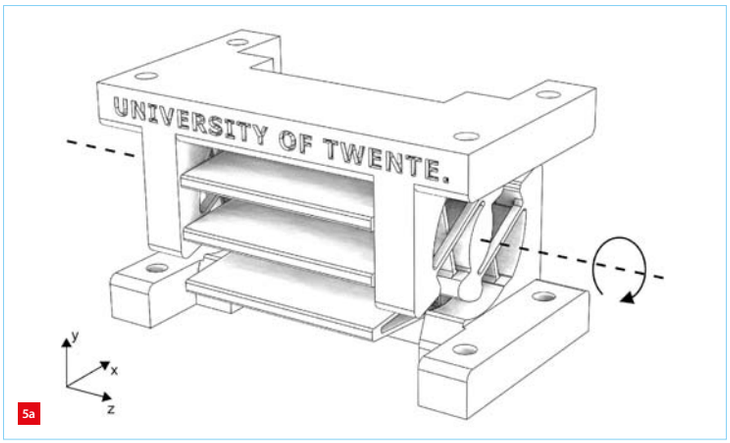

Appendix

Snapshots 'Multibody-based topology synthesis optimisation of a large-stroke flexure hinge' (Source: [5])

Iteration 1: LS & LS

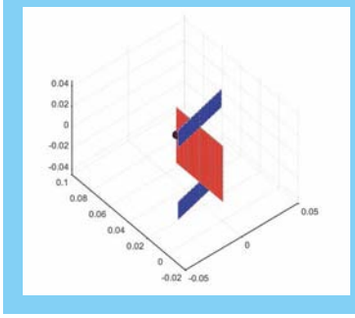

Iteration 2: TRLS (1x) & LS

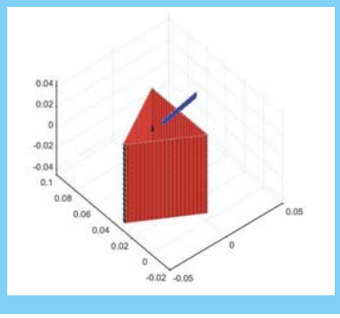

Iteration 3: TRLS (2x) & LS

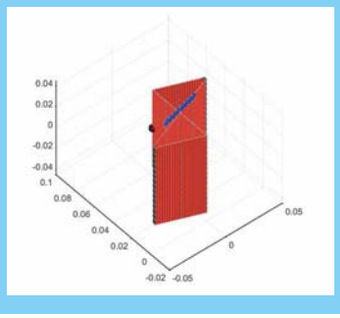

Iteration 4: TRLS (2x) & DTFCH

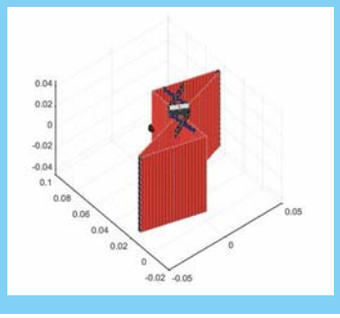

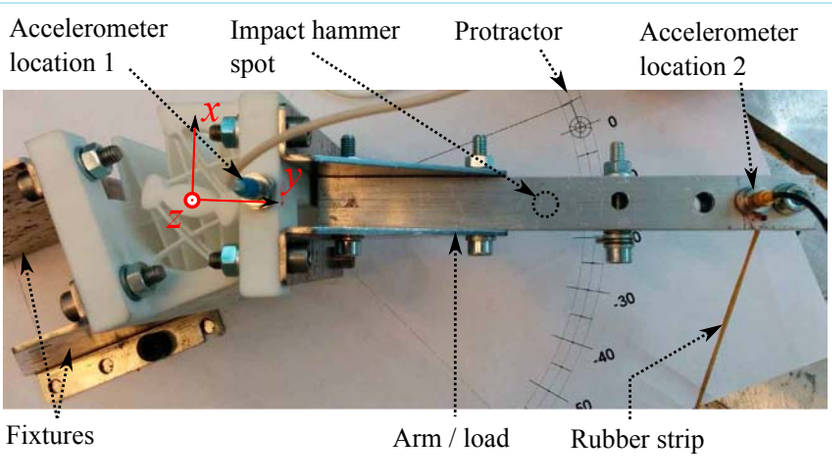

6

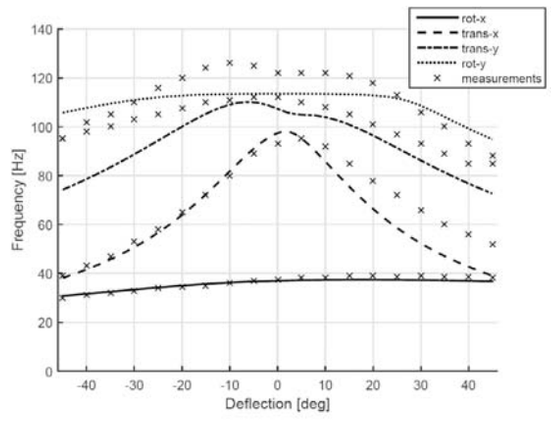

7

consisting of a rotation around the y-axis, shows a slight deviation in frequency. However, these deviations are within an acceptable range and only provide a positive increase in frequency. The deviations with respect to the experimental results can be explained by the interaction between modes with frequencies close to each other and the mixing of eigenmodes. Furthermore, possible inconsistencies in material properties and flexure thickness due to the sintering process can be of influence. The overall trend of the disturbing eigenfrequencies shows good agreement and confirm the models used, although the exact modeshape could only be confirmed for the first vibrational mode.

Conclusion

To effectively optimise topology for large-stroke flexure hinges, a new multibody-based topology synthesis method has been developed that combines a building-block-based layout variation strategy with a shape optimisation method in order to obtain the optimal topology. This method shows good results for optimising flexure hinges vastly exceeding the 10° range of motion and is capable of obtaining optimised solutions in a matter of hours.

The proposed method was used to design two flexure hinges for two selected applications, both of which resulted in a flexure design of unmatched performance. An optimisation case aimed at maximising support stiffness showed an increase in support stiffness of a factor eight with respect to the customary three-flexure cross hinge. In a second case, a flexure hinge was optimised to maximise parasitic frequency, which resulted in an increase in performance of a factor ten.

REFERENCES

[1] Jonker, J.B., Meijaard, J.P., "Spacar – computer program for dynamic analysis of flexible spatial mechanisms and manipulators", pp. 123-143 in Schiehlen, W. (ed.), *Multibody Systems Handbook*, Springer-Verlag, Heidelberg, 1990.

[2] Naves, M., Brouwer, D.M., Aarts, R.G.K.M., "Building block based spatial topology synthesis method for large stroke flexure hinges", *Journal of Mechanisms and Robotics*, 9(4), 2017.

[3] Wiersma, D.H., Boer, S.E., Aarts, R.G.K.M., Brouwer, D.M., "Design and Performance Optimization of Large Stroke Spatial Flexures", *Journal of Computational and Nonlinear Dynamics*, 9(1), 2013.

[4] Folkersma, K.G.P., Boer, S.E., Brouwer, D.M., Herder, J.L., Soemers, H.M.J.R., "A 2-dof Large Stroke Flexure based Position Mechanism", *IDETC ASME*, Chicago, IL, USA, Aug. 12-15, 2012.

[5] *www.youtube.com/watch?v=5scbEwPiq6Q*

6 *Measurement set-up for testing vibration modes at –20° deflection.*

7 *Experimental validation of the first four parasitic eigenfrequencies.*

Iteration 5: TRLS (3x) & DTFCH

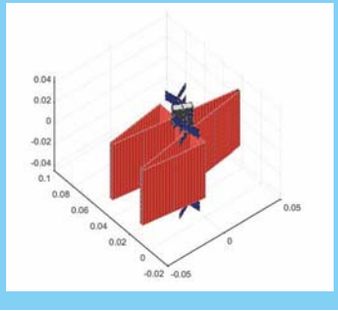

Iteration 6: TRLS (4x) & DTFCH

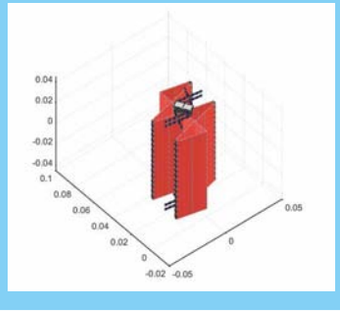

Iteration 7: TRLS (5x) & DTFCH

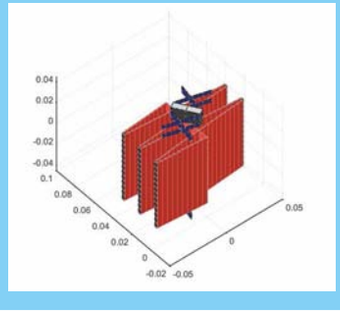

Iteration 8: TRLS (6x) & DTFCH